ELSEVIER

Journal of Nuclear Materials 280 (2000) 216–229

journal of nuclear materials

www.elsevier.nl/locate/jnucmat

Alteration kinetics of a simplified nuclear glass in an aqueous medium: effects of solution chemistry and of protective gel properties on diminishing the alteration rate

C. Jégou [a], S. Gin [a,*], F. Larché [b]

[a] *Commissariat à l'Énergie Atomique (CEA), Rhône Valley Research Center, DRRV/SCD, BP 171, 30207 Bagnols-sur-Cèze cedex, France*

[b] *Université de Montpellier II, Place E. Bataillon, GDPC CC26, 34095 Montpellier cedex 05, France*

Received 15 November 1999; accepted 28 February 2000

Abstract

The alteration kinetics of the French SON 68 nuclear glass simplified to its three major constituent elements (Si, B and Na) were investigated by static experiments at 90°C in order to deconvolute the effects of the solution chemistry and of the protective properties of the alteration gel on the diminishing alteration rate over time. A glass dissolution experiment in static conditions showed that the initial rate r_0 was maintained even after silicon saturation of the solution. As the reaction progressed, the glass alteration rate gradually diminished over time. These results show that the driving force behind the alteration of this glass cannot be defined by the difference from saturation with respect to amorphous silica, and that reaching saturation is not a criterion for the end of alteration. The drop in the dissolution rate observed at a high degree of reaction progress is correlated with the formation of the silica gel that develops at the glass/solution interface. Confronting the experimental data with a model taking into account a diffusion boundary layer shows that the conventional tools of chemical thermodynamics are ill adapted to describing the formation and development of the silica gel layer over time. This study reveals that only a dynamic process of hydrolysis and condensation of silicon at the glass/gel interface can account for the formation of the gel layer. The glass alteration rate under silica saturation conditions would thus be highly dependent on the silicon recondensation rate in this 'dynamic percolation' concept.

1. Introduction

Understanding the alteration mechanisms not only of nuclear borosilicate glasses but also of aluminosilicate (e.g. basaltic) glasses, which are natural analogs of nuclear glasses, is of considerable importance today in the perspective of a geological repository for vitrified nuclear waste packages.

Laboratory studies of the alteration kinetics of both types of glass have revealed several characteristic process steps [1–8]. The initial dissolution is characterized by ion exchange processes between protons in solution and glass network modifier cations, resulting in the formation of a hydrated layer depleted in alkali metal and alkaline earth cations, through which the aqueous species diffuse [9]. At the same time, the glass network consisting of network forming cations (Si, B, Al, etc.) hydrolyzes, causing the concentrations in solution to increase in a static system. As long as the medium remains sufficiently dilute, dissolution is congruent, i.e. all the elements are released at the reaction interface at the same rate. At a more advanced stage of the dissolution reaction, steady-state concentrations are observed – notably for the network formers – and the glass alteration rate is observed to diminish: dissolution then becomes incongruent. Both types of glass produce two sorts of alteration products: amorphous gels (known as palagonite for basaltic glass) and mineral phases (phyllosilicates, zeolites, calcium silicates, rare earth phosphates, etc.) [7,8,10,11].

* Corresponding author. Tel.: +33-4 66 79 14 65; fax: +33-4 66 79 66 20.

E-mail address: stephane.gin@cea.fr (S. Gin).

0022-3115/00/$ - see front matter
PII: S0022-3115(00)00039-8

The kinetic laws used to describe the dissolution of basaltic glass [6,12,13] and nuclear glass [14–17] are thus relatively similar, and almost always derived from the general law of mineral dissolution proposed by Aagaard and Helgeson in the early 1980s [18]

$$r_{\text{net}}^{\text{tot}} = k_{\min} \prod_i a_i^{-n_{i,j}} \left(1 - \exp\left(-\frac{A}{\sigma_j RT}\right)\right), \quad (1)$$

where $r_{\text{net}}^{\text{tot}}$ is the dissolution/precipitation rate of a mineral phase, $k_{\min}$ the kinetic constant of hydrolysis of the mineral, a_i the chemical activity of surface species i, $n_{i,j}$ the stoichiometric coefficient for reactant i in the limiting reaction j, R the ideal gas constant, T the temperature, A the chemical affinity of the overall dissolution/precipitation reaction, and σ_j is the stoichiometric coefficient of the elementary limiting reaction j in the overall reaction.

It should be noted that this type of kinetic law assigns considerable importance to the notions of chemical reaction affinity and saturation by taking into account either an alteration reaction based on an 'equilibrium' between the glass and solution [14] or an equilibrium between the gel and solution [19,20]. In other words, the glass dissolution kinetics are described based on the evolution of the concentrations in the homogeneous solution or at the (gel/solution) reaction interface of the chemical elements limiting the overall kinetics. However, other work has shown that borosilicate glasses of very similar composition exhibited strongly non-linear behavior with regard to the alteration kinetics at an advanced stage of reaction progress [21]. Recent experimental results [22] also revealed the renewed dissolution of a pristine glass specimen in an apparently saturated solution. Such behavior, which cannot be explained in terms of saturation, seems to depend on the protective effect of the gel formed during alteration.

These results notably demonstrate that it is essential to assess the respective contributions of the solution chemistry and of the protective properties of the gel in diminishing the glass dissolution rate, in order to develop a suitable kinetic formalism. A kinetic study was performed with a simple, homogeneous ternary (Si, B, Na) borosilicate glass composition situated below the percolation threshold to obtain additional data concerning this issue. The decision to use a simple glass of this type was fully justified by the fact that the principal kinetic models of nuclear glass alteration (GLASSOL in Germany, GLADISS in Switzerland, LIXIVER/PREDIVER in France) are based on Grambow's kinetic law, which takes only silicon into account. If the concepts postulated by Grambow are exact, they will thus be applicable to a ternary (Si, B, Na) glass, provided this type of glass exhibits the same reaction mechanisms as nuclear borosilicate glasses.

2. Experimental approach

2.1. Composition and fabrication of ternary (Si, B, Na) glass

The (Si, B, Na) glass sample, with a chemical composition corresponding to the elemental molar ratios of the French SON 68 (R7T7-type) nuclear glass, was fabricated in an induction-heated furnace by melting a mixture of SiO_2 (SIFRACO), H_3BO_3 (PROLABO) and Na_2CO_3 (PROLABO) in a platinum crucible at 1500°C and refining the melt for three hours. The glass was then poured into a preheated graphite mold and annealed for one hour at 590°C [23]. The furnace was switched off after annealing, and the glass was cooled slowly to room temperature.

The glass chemical composition (Table 1) was analyzed by ICP–AES after dissolving finely ground glass powder. Two types of alkaline melting procedures were used: NaOH–KNO_3 and lithium tetraborate. The glass density was determined using a hydrostatic balance: $\rho_g = 2.451(\pm 0.005)$ g cm^{-3}.

2.2. Homogeneity of ternary (Si, B, Na) glass

The ternary glass homogeneity was determined by Rayleigh–Brillouin light scattering. The Landau–Placzek ratio, R_{LP}, is usually defined by the relation

$$R_{\text{LP}} = \frac{I_{\text{R}}}{2I_{\text{B}}} \quad (2)$$

in which I_{R} is the intensity of the elastic component (Rayleigh scattering) and I_{B} is the intensity of the Brillouin line. It is used to detect crystallization or any other structural homogeneity defect (e.g. phase separation) exceeding about 50 Å that occurs during glass fabrication. Brillouin scattering was measured using a spectrometer equipped with a double-pass Fabry–Pérot plate interferometer; the light source was the 5145 Å green band produced by a 200 mW monomode ionized argon laser. All the measurements were performed at room temperature at right angles on $25 \times 25 \times 2$ mm^3 rectangular prismatic specimens with a high-grade (No. 4000) polished surface finish, with a surface roughness of less than 1 μm. The measured Brillouin shift and the R_{LP} value for the glass are indicated in Table 2. Each value

Table 1
Ternary (Si, B, Na) glass composition

	SiO_2	Na_2O	B_2O_3
Oxide weight percentage	65.56	14.21	20.23
Oxide molar percentage	67.73	14.23	18.04
	Si	Na	B
Elemental weight percentage	30.65	10.54	6.28

Table 2
Landau–Placzek ratio (R_{LP}) and Brillouin shift for ternary (Si, B, Na) glass and for silica

	(Si, B, Na) glass	Silica
R_{LP}	60 ± 5	50 ± 5
Brillouin shift	25.6 ± 0.2	

represents the mean of several separate determinations. The Landau–Placzek ratio measured for a silica specimen is also indicated for reference. It may be noted that the R_{LP} value for the ternary glass is on the same order of magnitude as for vitreous silica. No crystallization or segregation exceeding about 50 Å was observed; the glass was therefore homogeneous at this scale.

2.3. Leaching experiments

Ternary (Si, B, Na) glass powder samples were submitted to two types of alteration tests in initially pure water:

- a static test at 90°C (±1°C), at pH 9 (adjusted with 0.1N KOH) and at a low S/V ratio (0.1 cm^{-1}) to determine the initial alteration rate r_0;
- a static test at 90°C (±1°C), with an initial pH of 9 and at a high S/V ratio (4 cm^{-1}) to follow the Si, B and Na concentrations until silicon saturation conditions were reached.

The solution homogeneity was ensured by a magnetic stirring system; the pH (Orion combined electrode) and temperature were measured at regular intervals.

2.3.1. Powder preparation

Glass rods were ground to powder in a ball mill and screened to conserve the 40–100 μm size fraction. The powder sample was carefully washed in acetone to remove any residual fine grinding powder, then checked by SEM to ensure no fine particles remained on the powder grains. The specific area of the sample was determined by the BET (krypton) method to be 425 ± 4 cm^2 g^{-1}.

2.3.2. Initial rate measurement test

The experiments were conducted in a Teflon container containing 1000 ml of deionized water heated to 90°C; the pH was adjusted to 9 with a 0.1 mol l^{-1} KOH solution. The powder mass and solution volume in the reactor were then adjusted to obtain an S/V ratio of 0.1 cm^{-1}. Three-milliliter solution samples were taken with a syringe; each sample was filtered to 0.45 μm and acidified with 1N HNO_3 before ICP–AES analysis for Si, B and Na ($\leqslant 4\%$ precision). Samples were taken at short intervals (2, 4, 6, 8, 24, 30 and 48 h obtain the maximum number of data points in the initial stages of alteration.

2.3.3. Static test under silicon saturation conditions

The experiments were conducted in a Teflon container containing 250 ml of deionized water heated to 90°C. As in the initial rate experiments, the initial pH of the leaching solution was adjusted to 9 using a 0.1 mol l^{-1} KOH solution. The powder mass and solution volume in the reactor were then adjusted to obtain an S/V ratio of 4 cm^{-1}. Samples taken from the reactor were ultrafiltered to 10 000 daltons (corresponding to a cutoff threshold of 1.8 nm) before acidification. The samples were taken over a 14-day period (1, 2, 3, 4, 5, 6, 7, 8, 9, 10, 24, 48, 71, 95, 167 and 336 h). Two samples were taken at 336 h (one filtered to 0.45 μm, the second filtered to 0.45 μm then ultrafiltered) to assess the effect of the colloidal fraction on the silicon concentration measurements under saturation conditions.

2.3.4. Solution analysis results

2.3.4.1. Elemental normalized mass loss and silicon retention fraction in the alteration products. After correcting the concentration values for the effect of acid dilution, the normalized mass losses were calculated from the following relation:

$$NL_i = 10^{-2} \frac{C_i}{X_i \frac{S}{V}}, \tag{3}$$

where C_i is the concentration (mg l^{-1}) of element i in solution, S/V the glass surface-area-to-solution-volume ratio (cm^{-1}) and X_i is the mass fraction of element i in the glass. NL_i (expressed in g m^{-2}) is used to estimate the altered glass quantity when calculated for the mobile elements (B, Na), as well as to assess the retention of less mobile elements (notably Si) in the alteration products. SEM observation of the alteration films formed on this glass under silica saturation conditions has shown that the altered glass quantity can be determined from the boron concentration in solution [22].

The retention factor F_i for element i in the glass alteration products is defined with respect to boron (used as an alteration tracer) by the following relation:

$$F_i = 1 - \frac{NL_i}{NL_B}. \tag{4}$$

2.3.4.2. Altered glass percentage. The altered glass percentage is determined from the following relation:

$$AG\% = 10^{-4} \frac{C_B V}{m_0 X_B}, \tag{5}$$

where C_B is the boron concentration (mg l^{-1}), V the solution volume (ml), m_0 the initial powder mass (g) and X_B is the boron mass fraction in the glass.

2.3.4.3. Initial dissolution rate. Determining the initial dissolution rate. The initial glass dissolution rate

(g m^{-2} d^{-1}) with respect to element i is defined as follows:

$$r_0(i) = \frac{dNL_i}{dt}, \quad (6)$$

where NL_i is expressed in g m^{-2}. During the time interval in which the concentrations vary in a linear manner, the rates are calculated by linear regression from the normalized elemental mass loss values.

Initial dissolution rate and percolation. The NL_{Si}/NL_B and NL_{Na}/NL_B congruence ratios during the initial stages of alteration are significant indicators of the relation between the glass composition and the percolation threshold. In glass compositions situated above the percolation threshold, the soluble elements (boron and the alkali metals) can be quickly solubilized before the remainder of the network is altered by the slower dissolution of silica (i.e. selective dissolution). For the other glass compositions, after release of the soluble elements near the surface, dissolution is congruent and controlled by the dissolution of silica. As discussed below, the ternary glass investigated in this study was situated below the percolation threshold.

2.3.4.4. Shrinking core model. In the case of strongly altered samples, the reactive surface area must be corrected during the experiment. A 'shrinking core' model (see Appendix A) is used to take into account the changing S/V ratio over time. This type of correction was used for the 4 cm^{-1} leaching experiment.

3. Experimental results

3.1. Initial dissolution rate

The normalized mass losses for silicon, boron and sodium between 2 and 48 h of alteration under static conditions at 90°C and pH 9 are indicated in Fig. 1, which shows the relatively congruent dissolution rates for the three elements during the initial alteration period. This in turn implies that the test glass is well below the percolation threshold, and that the dissolution of these elements is indeed controlled by the silica dissolution rate. Moreover, as the normalized mass losses vary in a linear manner during the first 48 h, the initial dissolution rate can be calculated in the absence of any alteration film by linear regression from the elemental mass loss values: $r_0 = 4.5 \pm 1$ g m^{-2} d^{-1}. At the same temperature and pH, the initial dissolution rate of the French SON 68 (R7T7-type) nuclear glass is 2 g m^{-2} d^{-1} [7].

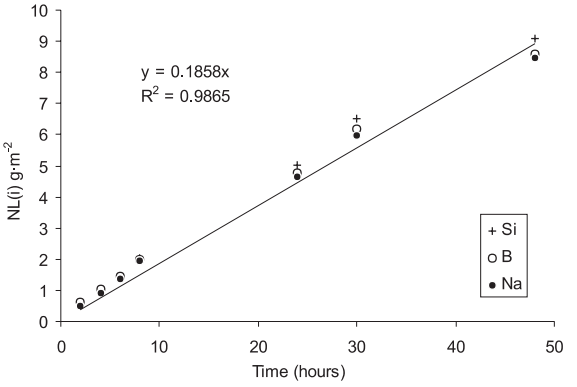

Fig. 1. Normalized silicon, boron and sodium mass losses versus time during the first 48 h of glass alteration under static conditions at 90°C, pH 9 and S/V 0.1 cm^{-1}. The relative uncertainty on NL_i was estimated at 5%. Glass dissolution was congruent under these conditions.

3.2. Test results under silica saturation conditions

The solution analysis results for the static tests at S/V 4 cm^{-1} are listed in Table 3.

Fig. 2 shows the evolution of the normalized mass losses for silicon, boron and sodium during the first 24 h, after which saturation with respect to amorphous silica was reached in the homogeneous solution (see Table 4). The most significant result of this test is that the glass continued to dissolve at the maximum (initial) rate r_0 until saturation occurred with respect to amorphous silica. Fig. 2 shows that dissolution remained congruent for boron and sodium throughout the 24-h period,

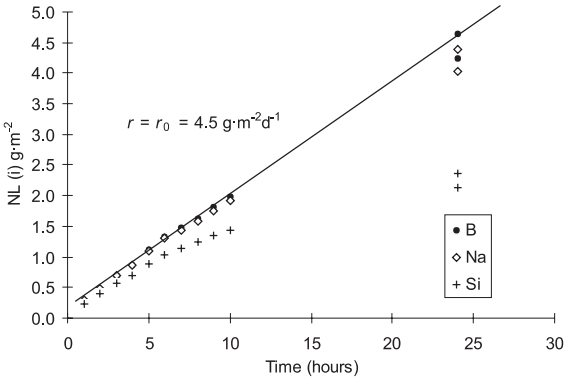

Fig. 2. Normalized silicon, boron and sodium mass losses versus time during the first 24 h of glass alteration under static conditions at 90°C, pH 9 and S/V 4 cm^{-1}. The relative uncertainty on NL_i was estimated at 5%. The overall glass dissolution became incongruent after the first 3 h due to the formation of the silica gel.

Table 3
Solution analysis data for ternary (Si, B, Na) glass alteration under static conditions at 90°C, pH 9 and S/V 4 cm^{-1} [a]

Time (h)	pH (90°C)	Si (mg l^{-1})	B (mg l^{-1})	Na (mg l^{-1})	AG%	V (ml)	S/V (cm^{-1})	NL(Si) (g m^{-2})	NL(B) (g m^{-2})	NL(Na) (g m^{-2})	F_{Si}	F_{Na}
1	8.96	28.5	6.9	12.4	1.1	250	4.01	0.23	0.28	0.29	0.16	–0.07
2	nd	49.0	11.9	20.5	2.0	249	3.99	0.40	0.47	0.49	0.16	–0.03
3	nd	70.5	17.8	30.0	2.9	248	3.99	0.58	0.71	0.71	0.19	0.00
4	nd	86.4	22.2	36.9	3.6	247	3.98	0.71	0.89	0.88	0.20	0.01
5	8.81	110.0	28.6	46.9	4.6	246	3.98	0.90	1.14	1.12	0.21	0.02
6	nd	128.8	33.9	55.5	5.5	245	3.96	1.06	1.36	1.33	0.22	0.02
7	8.8	140.7	37.3	61.1	6.0	244	3.96	1.16	1.50	1.46	0.23	0.02
8	nd	153.0	41.2	67.3	6.6	243	3.96	1.26	1.66	1.61	0.24	0.03
9	nd	166.1	46.1	74.8	7.4	242	3.96	1.37	1.86	1.79	0.26	0.03
10	8.8	177.7	50.2	82.0	8.0	241	3.95	1.47	2.02	1.97	0.27	0.03
24	8.86	264.3	107.5	171.3	17.0	240	3.95	2.18	4.33	4.11	0.50	0.05
24	nd	274.0	110.1	174.8	17.4	239	3.70	2.41	4.73	4.48	0.49	0.05
47	8.95	221.9	188.4	280.5	29.6	238	3.71	1.95	8.09	7.18	0.76	0.11
71	8.95	322.3	231.3	347.8	36.2	237	3.35	3.14	11.01	9.86	0.71	0.10
95	9.03	324.2	262.7	396.3	41.0	236	3.15	3.36	13.29	11.95	0.75	0.10
167	9.03	301.3	294.3	437.7	45.7	235	3.00	3.27	15.61	13.84	0.79	0.11
336	9.07	312.5	323.6	488.9	50.0	234	2.85	3.58	18.07	16.27	0.80	0.10
336[b]	9.07	334.2	337.1	501.3	51.9	233	2.71	4.03	19.82	17.56	0.80	0.11

[a] The pH values were measured at 90°C; the altered glass percentages (AG%) were calculated from the boron concentrations (Eq. (5)); the S/V ratios were corrected for the strong powder grain alteration by means of a shrinking core model (Appendix A); the normalized mass losses were calculated from Eq. (3), and the silicon and sodium retention factors in the gel from Eq. (4).
[b] The final analysis was performed on a solution filtered to 0.45 μm; comparison with the ultrafiltered solution analysis for the same interval shows a 7% difference in the Si concentration, which may be considered near the analytical uncertainty.

Table 4
pH, total silicon concentration and H_4SiO_4 concentration in solution during dissolution of ternary (Si, B, Na) glass at 90°C, pH 9 and S/V 4 cm^{-1} [a]

Time (h)	pH	C_{si} (mg l^{-1})	log $C_{H_4SiO_4}$
1	8.96	28.5	–3.29
5	8.81	110.0	–2.64
7	8.80	140.7	–2.53
10	8.80	177.7	–2.42
24	8.86	274.0	–2.26

[a] The calculated H_4SiO_4 concentration after 24 h corresponds to the solubility of amorphous silica [34].

whereas the silicon dissolution rate dropped significantly after only a few hours. This result – which was not observed at the lower S/V ratio (0.1 cm^{-1}) because of the short leaching time – implies that a fraction of the silicon was retained at the reaction interface even though the homogeneous solution was not yet saturated with respect to amorphous silica. SEM observations after 0.5 day clearly revealed the formation of silica spherules at the glass/solution reaction interface (Fig. 3(a)), although the silicon concentration in solution did not exceed 180 mg l^{-1} (compared with the saturation value of 274 mg l^{-1} at pH 8.9). The calculated silicon retention factors in the alteration film (Table 3) indicate that 20% of the silicon was retained at the reaction interface after only 2–3 h of alteration.

The evolution of the normalized mass losses for silicon, boron and sodium over the first 14 days is shown in Fig. 4. Although neither the silica gel nor the solution chemistry had any effect on the alteration rate during the first 24 h, Fig. 4 clearly shows a drop in the alteration rate occurring 2–3 days after saturation. The mean alteration rate calculated between 7 and 14 days from the boron mass loss ($r = \Delta NL_B/\Delta t = 0.35$ g m^{-2} d^{-1}) reveals that the alteration rate dropped by about an order of magnitude from the initial rate r_0. At the same time the glass alteration rate diminished, the coverage of the surface by silica spherules increased (Fig. 3(b)).

4. General discussion and modeling

Both experiments conducted with the (Si, B, Na) glass show that its reaction kinetics are similar to those described for the SON 68 nuclear glass [8,22,24]. At the same temperature and pH, the measured initial rates are comparable (4.5 g m^{-2} d^{-1} for the simplified glass and 2 g m^{-2} d^{-1} for the nuclear glass) and in highly dilute media both glasses dissolve congruently. At high S/V ratios, both glasses show steady-state Si concentrations and alteration rates that gradually diminish over time. These similarities justify the application to a simple (Si, B, Na) glass of kinetic models developed for nuclear glasses [14–17,19].

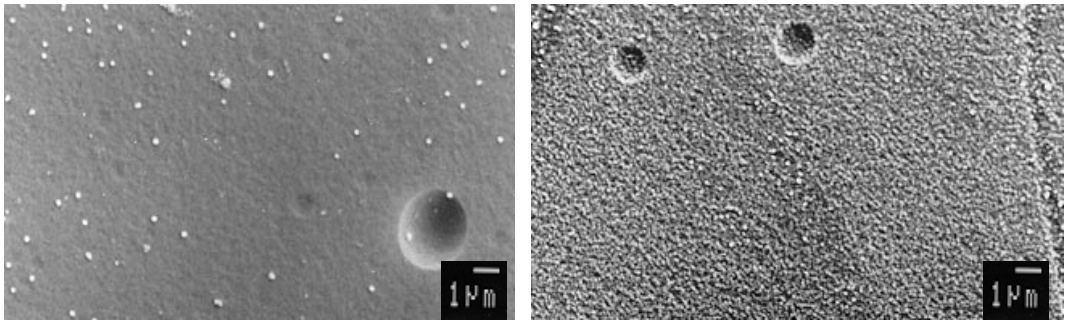

Fig. 3. Scanning electron micrograph (15 kV) of the altered glass surface (S/V 4 cm^{-1}): (a) after 0.5 day of alteration; (b) after 7 days of alteration. The number of amorphous silica spherules (gel precursors) at the interface increased during the glass alteration reaction.

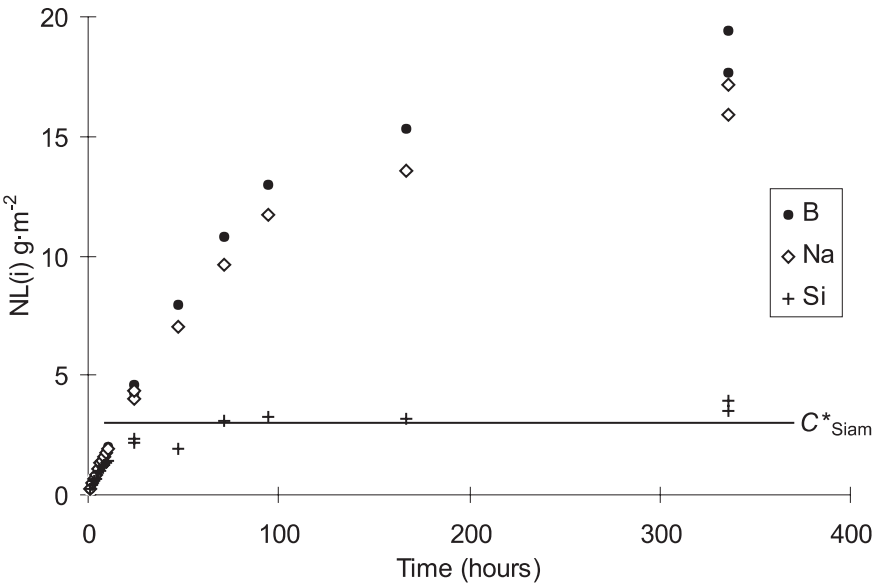

Fig. 4. Normalized silicon, boron and sodium mass losses versus time during the first 14 days of glass alteration under static conditions at 90°C, pH 9 and S/V 4 cm^{-1}. After about 50 h, the glass alteration rate (determined from the boron and sodium release) gradually diminished to approximately $r_0/10$ after 14 days.

4.1. Describing the diminishing (Si, B, Na) glass alteration rate in terms of a chemical affinity function

Various kinetic laws have been proposed in the literature [14–17,19] to account for the drop in the alteration rate observed for nuclear borosilicate glasses. All these kinetic approaches associate the glass alteration rate drop with a deviation from 'equilibrium' between the glass (or alteration film) and solution. Three of them can be compared with the experimental results of this study: all three were derived from the general law of mineral dissolution (Eq. (1)) proposed by Aagaard and Helgeson in the early 1980s [18].

4.1.1. Grambow's model

In the model proposed by Grambow [14], the glass dissolution reaction is limited to the following:

$$(SiO_2)_{glass} + 2H_2O \rightarrow H_4SiO_4. \tag{7}$$

The Aagaard–Helgeson law is then expressed as follows:

$$r = r_0\left(1 - \frac{a^{int}_{H_4SiO_4}}{a^*}\right), \tag{8}$$

where r_0 is the initial glass dissolution rate depending only on the pH and temperature, $a^{int}_{H_2SiO_4}$ is the orthosilicic

acid activity at the reaction interface, and a^* is the orthosilicic acid activity at saturation with the glass.

Applying a first-order law, based on the orthosilicic acid activity at the glass/solution reaction interface, to our experimental work would imply that the alteration rate diminishes when the solution becomes concentrated with silicon. In our study, however, no drop in the alteration rate was observed under these conditions. Grambow's model cannot be eliminated altogether on the basis of this experiment, since if the glass 'solubility' were much higher than that of amorphous silica, the measured silicon concentrations would be too low to diminish the alteration rate. Nevertheless, Grambow's model alone cannot account for the drop in the alteration rate observed under saturation conditions with the (Si, B, Na) glass.

4.1.2. Coupling Grambow's model with water diffusion in the glass

Another hypothesis advanced by Grambow postulates an equilibrium between the glass and solution, together with a water diffusion mechanism in the glass (Grambow, personal communication). This hypothesis would suggest that the solubility of the (Si, B, Na) glass exceeds that of amorphous silica, since the glass alteration rate remained at its initial value until the solution became saturated. The affinity effect would therefore be negligible, and the glass alteration rate would be controlled only by diffusion of water in the glass. This might not appear to be a pertinent assumption, inasmuch as the glass alteration rate at silica saturation should not depend on the available glass reactive surface area. However, comparing the glass alteration rates measured at various S/V ratios between the moment when the solution is saturated and a given sampling interval (e.g. 14 days) shows that the rate clearly depends to a large extent on the S/V ratio: 0.8 g m^{-2} d^{-1} at 4 cm^{-1} versus 0.09 g m^{-2} d^{-1} at 80 cm^{-1} [22]. This result pleads for the glass alteration rate being controlled by the rate at which the hydrolyzed species recondense, which in turn depends on the number of available recondensation sites and thus on the S/V ratio.

4.1.3. The Aagaard–Helgeson law

The Aagaard–Helgeson law [18] requires that the overall glass dissolution reaction be taken into account. A very general formulation is the following:

glass $+ n\mathrm{H_2O} \rightarrow$ hydrolyzed species.

The ion activity product Q is calculated in this case from the activities in solution of all the hydrolyzed species produced during the reaction. Even if sodium and boron are highly soluble and should not affect the diminishing (Si, B, Na) glass alteration rate, the drop in the rate $(r/r_0 = 1 - Q/K)$ can be estimated from a thermodynamic model based on the free standard enthalpy of glass hydration [25,26].

Paul's and Jantzen's models. In the models proposed by Paul [25] or by Jantzen and Plodinec [26], the free enthalpy of hydration of an oxide glass is calculated by considering the glass as a solid and ideal solution of simple oxides (SiO_2, Al_2O_3, etc.) and silicates ($ZrSiO_4$, Na_2SiO_3, etc.). The free enthalpy of hydration is then expressed as an additive function of the free enthalpies of hydration of each of the silicates and simple oxides [25]

$$\Delta G^0_{\mathrm{hydrat}} = \sum_i x_i \Delta G^0_{\mathrm{hydrat},i} \tag{9}$$

or as follows, with a slight correction for the entropy of the mixture [26]

$$\Delta G^0_{\mathrm{hydrat}} = \sum_i x_i \Delta G^0_{\mathrm{hydrat},i} + RT \sum_i x_i \ln x_i, \tag{10}$$

where x_i is the molar fraction corresponding to the silicate or simple oxide i, and $\Delta G^0_{\mathrm{hydrat},i}$ is the standard free enthalpy of hydration associated with a simple reaction of the type

$\mathrm{M_xO_y} + \mathrm{H_2O} \leftrightarrow$ hydrated species.

The structural entities and hydrolyzed species we considered for the ternary (Si, B, Na) glass are listed in Table 5 together with the standard free enthalpy of hydration for the simple ($\mathrm{M_xO_y} + \mathrm{H_2O} \leftrightarrow$ hydrated species) reactions. Unlike silica and boron, the free enthalpy of formation considered for Na_2SiO_3 is that of the corresponding crystalline phase. The free standard enthalpy values were determined at 90°C based on the thermodynamic data of the Nuclear Energy Agency (NEA) and on the data proposed in the literature [25,26]. The data were also extrapolated to 25°C using the van't Hoff relation

$$\log K(T) = \log K(T_{\mathrm{r}}) - \frac{\Delta H^0_{\mathrm{r}}(T_{\mathrm{r}})}{2.303R}\left(\frac{1}{T} - \frac{1}{T_{\mathrm{r}}}\right), \tag{11}$$

Table 5
Simple reactions considered to calculate the free enthalpy of hydration of the (Si, B, Na) glass

Hydration reaction	Free enthalpy of hydration at 90°C (kcal mol^{-1})	log K at 90°C
$SiO_2 + 2H_2O \rightarrow H_4SiO_4$	3.87	−2.33
$B_2O_3 + 3H_2O \rightarrow 2B(OH)_3$	−8.67	5.22
$Na_2SiO_3 + H_2O + 2H^+ \rightarrow 2Na^+ + H_4SiO_4$	−32.00	19.22

where T_r is the reference temperature (298.15 K), T the reaction temperature, and ΔH_r^0 is the standard reaction enthalpy.

In this thermodynamic model, the overall dissolution reaction for the ternary (Si, B, Na) glass is then written as follows:

$$0.535\ SiO_2 + 0.180\ B_2O_3 + 0.284\ H^+ + 0.142\ Na_2SiO_3 + 1.753\ H_2O \rightarrow 0.360\ B(OH)_3 + 0.677\ H_4SiO_4 + 0.284\ Na^+. \quad (12)$$

Thus $\Delta G^0_{hydrat} = -4.02$ kcal mol^{-1} and $\log K_{glass} = 2.41$. Correcting for the mixture entropy yields $\log K_{glass} = 2.02$.

Having evaluated $\log K_{glass}$ and knowing the silicon, boron and sodium concentrations in solution, we can now estimate the drop in the alteration rate ($r/r_0 = 1 - Q/K$) for the (Si, B, Na) glass at a given instant during the leaching experiment. Calculating the ion activity product $Q = a^{0.360}_{B(OH)_3} a^{0.677}_{H_4SiO_4} a^{0.248}_{Na^+} a^{-0.284}_{H^+}$ provides an easy method for verifying that $r/r_0 \cong 1$ at each sampling interval during the experimental period.

Contribution of the model. Paul's model, when applied to our kinetic study, mainly provided an indication of the expected effect of boron and sodium on the reduction of the glass alteration rate. It furnished additional arguments concerning the inadequacy of a kinetic law based on a chemical affinity function describing a deviation from 'equilibrium' between the glass as a whole and the solution. The quantitative aspect of this kinetic model calls for some reserves, however, since Paul's model notably does not take into account the energy necessary for vitrification.

4.1.4. Bourcier's model

Bourcier [19] proposed a model that did not postulate any 'equilibrium' between the glass and solution. The glass alteration rate is assumed to follow a gel dissolution chemical affinity function of the type $(1-Q/K)$ calculated from the gel composition. The authors justify their approach by advancing the hypothesis that once the steps leading to the release of the cations from the glass and to hydrolysis of the silicate bonds (forming silanol groups) have occurred, the structure very quickly reforms through silanol condensation reactions. The gel thus formed then reacts again with water at the water/gel interface, releasing orthosilicic acid into solution. The limiting step in glass alteration is thus not the conversion of the glass into a gel, but the gel dissolution kinetics. The thermodynamic properties of the gel are defined by considering the gel as an ideal solid solution of amorphous phases and hydroxides.

The alteration experiment conducted at an S/V ratio of 4 cm^{-1} invalidates Bourcier's model. The alteration film formed during this experiment was a pure silica gel corresponding to the simplest possible situation in Bourcier's model, which implies that the kinetics cease when the gel reaches equilibrium with the homogeneous solution. In this case, there was indeed an equilibrium between the gel and the homogeneous solution, but this condition proved insufficient to slow – much less stop – the alteration kinetics.

4.1.5. Conclusion

The drop in the alteration rate observed over sufficiently long periods cannot be interpreted using only classic kinetic laws based on chemical thermodynamic concepts (solubility, chemical affinity function, etc.). In the case of the simple glass investigated here, only an effect associated with the formation of the silica gel (a diffusion barrier) can account for the observed drop in the alteration rate under silica saturation conditions. This conclusion regarding the protective effect of the gel corroborates the findings of many other studies of nuclear glasses [22,27–30].

4.2. Gel formation mechanisms

The following paragraphs consider the mechanisms by which the silica gel forms on the (Si, B, Na) glass.

4.2.1. Boundary-layer model

A possible hypothesis for the formation of the silica gel is that the solubility of the precipitating phase is reached at the reaction interface. In this approach, the time necessary to reach saturation with respect to amorphous silica in the boundary layer must be determined. This calculation is based on the following assumptions:

- the powder grain radius variation is small enough (≈2% up to 24 h) to be compatible with plane geometry;
- the glass dissolution rate is constant (r_0);
- silicon diffuses into solution with no significant electrical effect (e.g. as H_4SiO_4).

4.2.1.1. Symbols and numerical values.

C^{int}_{Si} max	highest silicon concentration at the reaction interface mg l^{-1}
C^{int}_{Si}	silicon concentration at the reaction interface mg l^{-1}
C_{Si}	silicon concentration in the homogeneous solution mg l^{-1}
d	mean distance between glass powder grains 155 μm
D	diffusion coefficient in the liquid medium 2.5×10^{-9} m^2 s^{-1}
q	ratio of solution volume to boundary layer volume 69.75 (dimensionless)
R	glass powder grain radius 33.7 μm

r_0	initial alteration rate 4.5 g m^{-2} d^{-1} (5.2×10^{-5} g m^{-2} s^{-1})
S/V	ratio of glass surface area to solution volume 4 cm^{-1}
V	solution volume 250 ml
T	test temperature 363 K
t_1	diffusion time constant in boundary layer 0.24 s
v_∞	velocity in solution due to stirring 0.1 m s^{-1}
δ	boundary layer thickness 35 μm
μ	fluid viscosity 0.3145 mPa s
ρ	liquid density 0.965 g cm^{-3}
ρ_g	glass density 2.45 g cm^{-3}
Ψ	silicon mass fraction in the glass 0.306

4.2.1.2. Formation of a boundary layer. In a lightly stirred solution, we postulate that a diffusion boundary layer forms in which there is a constant concentration gradient (only silicon is considered in the following discussion). This condition occurs after a transient phase whose duration we intend to estimate. If δ is the boundary layer thickness and D is the diffusion coefficient of the siliceous species, then the penetration time over this distance is

$$\tau = \frac{\delta^2}{4D}. \tag{13}$$

The time necessary to reach linear conditions is about three or four times τ. Estimating a numerical value requires a prior estimate of the boundary layer thickness. The mean distance between grains during alteration constitutes an upper limit. The number of presumed spherical powder grains in 250 ml of solution is about 6 million; assuming a cubic face-centered lattice with four grains per unit cell, the cell parameter is

$$a = \left(\frac{4V}{N}\right)^{1/3} \tag{14}$$

and the distance between grains is

$$d = \frac{a}{\sqrt{2}}. \tag{15}$$

Hence $\delta = 380$ μm. The boundary layer thickness is certainly less than half the difference between the grain surfaces, i.e.

$$\delta \leqslant \frac{d-2R}{2}, \tag{16}$$

where R is the mean grain radius. The numeric solution is

$$\delta \leqslant 155\ \mu\text{m}. \tag{17}$$

With a simple cubic lattice, a similar calculation gives a value of 140 μm.

Another estimate can be obtained by calculating a velocity boundary layer, assuming negligible mass transfer [31]. We considered the thickness of the layer formed on a flat surface at a distance l from the edge, in a fluid with an unimpeded velocity v_∞

$$\delta = \sqrt{12\frac{\mu l}{\rho v_\infty}}, \tag{18}$$

where μ is the fluid viscosity and ρ the fluid density. In water at 90°C, $\rho = 0.965$ g cm^{-3} and $\mu = 0.3145$ mPa s [32]. Allowing for the effect of stirring in the reactor, the velocity v_∞ may be estimated at 0.1 m s^{-1}. The boundary layer thickness would then be $\delta = 35$ μm.

The time required to reach linear conditions can be calculated using the diffusion coefficient, which may be estimated from the Stokes–Einstein formula

$$D = \frac{k_B T}{6\pi\mu R_H}, \tag{19}$$

where k_B is the Boltzmann constant, T the absolute temperature, and R_H is the hydrodynamic radius of the diffusing particle – for which we adopted a value of 0.35 nm [33] – resulting in a diffusion coefficient of 2.5×10^{-9} m^2 s^{-1} at 90°C. The time τ calculated using these values is then 0.12 s.

The duration of the transient phase leading to the establishment of a linear concentration profile in the boundary layer is thus less than one second. The concentration reached at the surface after this time is approximated by the following formula:

$$C_{Si}^{int} = \frac{2r_0\psi t}{\delta}. \tag{20}$$

With the experimentally determined numeric values, the resulting silicon concentration is thus $C_{Si}^{int} = 0.11$ mg l^{-1}, a value well below saturation with respect to amorphous silica (320 mg l^{-1} at pH 9 [34]). For the purposes of the following discussion, it will be assumed to be practically zero.

4.2.1.3. Evolution of the boundary layer. After the transient phase described above, we shall assume that the concentration gradient remains constant throughout the boundary layer, and that its evolution over time can be calculated as follows (the concentrations are C_{Si}^{int} at the glass/boundary layer interface and C_{Si} in solution (Fig. 5)).

Initially, we shall simplify the equations by assuming the concentration in solution remains practically nil; this constraint will be eliminated later. A silicon balance in the boundary layer can be established as follows:

- silicon input through diffusion

$$DS\frac{C_{Si}^{int}}{\delta}dt. \tag{21}$$

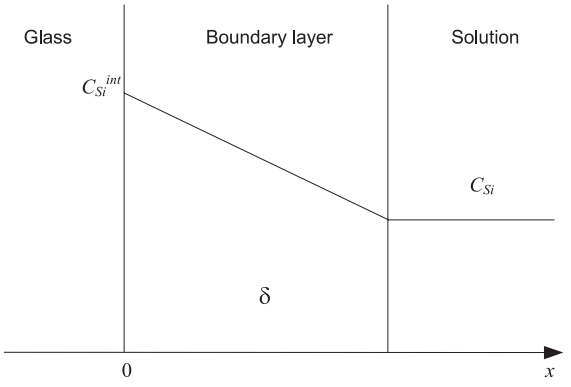

Fig. 5. Boundary layer adjacent to the alteration front; the axes are mobile, with the origin situated at the alteration front.

- evolution of the quantity of silicon in the boundary layer

$$S\frac{\delta}{2}\frac{\mathrm{d}C_{\mathrm{Si}}^{\mathrm{int}}}{\mathrm{d}t}\mathrm{d}t. \tag{22}$$

The balance is thus

$$r_0\psi - D\frac{C_{\mathrm{Si}}^{\mathrm{int}}}{\delta} = \frac{\delta}{2}\frac{\mathrm{d}C_{\mathrm{Si}}^{\mathrm{int}}}{\mathrm{d}t}. \tag{23}$$

As noted above, the initial condition is $C_{\mathrm{Si}}^{\mathrm{int}}(0) = 0$.

The solution to the differential equation is thus

$$C_{\mathrm{Si}}^{\mathrm{int}} = \frac{r_0\psi\delta}{D}\left(1 - \mathrm{e}^{-2D/\delta^2 t}\right). \tag{24}$$

The concentration rises from zero at $t = 0$ to reach the maximum value

$$C_{\mathrm{Si}}^{\mathrm{int}}\,\mathrm{max} = \frac{r_0\psi\delta}{D}. \tag{25}$$

Substituting the previously mentioned values yields

$C_{\mathrm{Si}}^{\mathrm{int}}\,\mathrm{max} = 0.22\ \mathrm{mg\ l^{-1}}$.

The model is therefore incapable of reaching a concentration in the boundary layer corresponding to saturation with respect to amorphous silica. This situation can be modified by allowing for a rising silica concentration in solution; under these conditions, the gradient – and thus the outward flow from the boundary layer – will be lower. The differential equations describing the evolution of concentrations $C_{\mathrm{Si}}^{\mathrm{int}}$ and C_{Si} are obtained as above, by establishing a balance for the boundary layer.

- Silicon input through glass alteration during the time interval dt

$$Sr_0\psi\,\mathrm{d}t. \tag{26}$$

- Silicon output by diffusion and shifting of the interface position

$$DS\frac{C_{\mathrm{Si}}^{\mathrm{int}} - C_{\mathrm{Si}}}{\delta}\mathrm{d}t + C_{\mathrm{Si}}S\frac{r_0}{\rho_v}\mathrm{d}t. \tag{27}$$

- Evolution of the quantity of silicon in the boundary layer

$$S\frac{\delta}{2}\left(\frac{\mathrm{d}C_{\mathrm{Si}}^{\mathrm{int}}}{\mathrm{d}t} + \frac{\mathrm{d}C_{Si}}{\mathrm{d}t}\right)\mathrm{d}t. \tag{28}$$

- Evolution of the concentration in solution:

$$V\frac{\mathrm{d}C_{\mathrm{Si}}}{\mathrm{d}t}\mathrm{d}t. \tag{29}$$

The silicon balances in the boundary layer and in solution yield the desired equations

$$\frac{D}{\delta}C_{\mathrm{Si}}^{\mathrm{int}} + \left(\frac{r_0}{\rho_v} - \frac{D}{\delta}\right)C_{\mathrm{Si}} + \frac{\delta}{2}\frac{\mathrm{d}C_{\mathrm{Si}}^{\mathrm{int}}}{\mathrm{d}t} + \frac{\delta}{2}\frac{\mathrm{d}C_{\mathrm{Si}}}{\mathrm{d}t} = r_0\psi, \tag{30}$$

$$\frac{D}{\delta}C_{\mathrm{Si}}^{\mathrm{int}} + \left(\frac{r_0}{\rho_v} - \frac{D}{\delta}\right)C_{\mathrm{Si}} - \frac{V}{S}\frac{\mathrm{d}C_{\mathrm{Si}}}{\mathrm{d}t} = 0. \tag{31}$$

The initial conditions are the same as in the preceding example: $C_{\mathrm{Si}}^{\mathrm{int}}(0) = 0$ and $C_{\mathrm{Si}}(0) = 0$.

The result is similar to the previous equation when V is very large compared with S. Before attempting to solve this linear differential equation system, it may be simplified by considering the order of magnitude of the coefficients: thus $D/\delta = 7.4 \times 10^{-5}$ m s^{-1}, whereas $r_0/\rho_v = 2.11 \times 10^{-11}$ m s^{-1}. The second term is negligible compared with the first. Physically, this indicates that the entry of silicon into solution is due only to diffusion. If we then define a time constant (i.e. for diffusion through the boundary layer)

$$t_1 = \frac{\delta^2}{2D} \tag{32}$$

and the ratio between the solution volume and the boundary layer volume

$$q = \frac{V}{S\delta} \tag{33}$$

the above-defined equation system then becomes

$$C_{\mathrm{Si}}^{\mathrm{int}} + C_{\mathrm{Si}} + t_1\frac{\mathrm{d}C_{\mathrm{Si}}^{\mathrm{int}}}{\mathrm{d}t} + t_1\frac{\mathrm{d}C_{\mathrm{Si}}}{\mathrm{d}t} = C_{\mathrm{Si}}^{\mathrm{int}}\,\mathrm{max}, \tag{34}$$

$$C_{i\mathrm{Si}}^{\mathrm{int}} + C_{\mathrm{Si}} - 2qt_1\frac{\mathrm{d}C_{\mathrm{Si}}}{\mathrm{d}t} = 0 \tag{35}$$

with the following solution for the initial conditions:

$$C_{\mathrm{Si}}^{\mathrm{int}} = C_{\mathrm{Si}}^{\mathrm{int}}\,\mathrm{max}\left[\frac{t}{2qt_1} + \frac{q(1+2q)}{2(q+1)^2}\left(1 - \mathrm{e}^{-q+1/qt_1}\right)\right], \tag{36}$$

$$C_{\mathrm{Si}} = C_{\mathrm{Si}}^{\mathrm{int}}\,\mathrm{max}\left[\frac{t}{2(q+1)t_1} + \frac{q}{2(q+1)^2}\left(\mathrm{e}^{-q+1/qt_1} - 1\right)\right]. \tag{37}$$

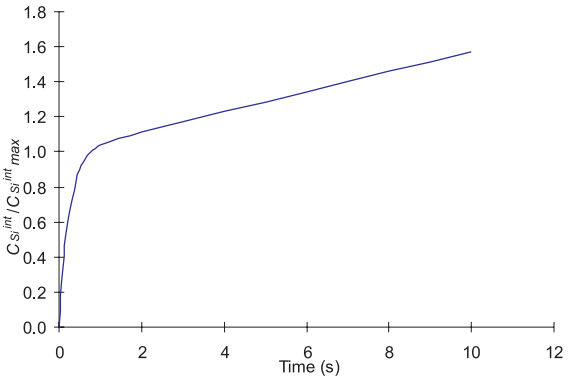

Fig. 6. Relative concentration $C_{Si}^{int}/C_{Si}^{int}$ max versus time.

In the particular example considered here, these equations may be simplified by noting that $q = 69.75$. Considering 1 to be negligible with regard to q, the expressions are then

$$C_{Si}^{int} \approx C_{Si}^{int}\,\max\left[\frac{t}{2qt_1} + 1 - e^{-t/t_1}\right], \tag{38}$$

$$C_{Si} \approx C_{Si}^{int}\left[\frac{t}{2qt_1} + \frac{1}{2q}\left(e^{-t/t_1} - 1\right)\right]. \tag{39}$$

This approximation corresponds to the preceding solution for C_{Si}^{int} with the addition of a linear term, i.e. two regimes as indicated in Fig. 6.

The concentration rises quickly during the first 0.6 s; from about 1 s onward, the concentration at the reaction interface rises linearly. Even in this model, saturation with respect to amorphous silica is reached only after a very long time (some 13 h), in contradiction with the experimental findings indicating a divergence between boron and silicon in the first samples (2–3 h). Under the conditions of this experiment, Eq. (24) is thus largely sufficient for a discussion of the model.

4.2.1.4. Boundary-layer model: discussion and conclusion. The formation of a passivation layer during oxidation of some metals is generally attributed to the onset of saturation with respect to an oxide or a hydroxide at the reaction surface [35]. We considered applying a model of this type to alteration of our (Si, B, Na) glass, and found that saturation with respect to amorphous silica in the grain boundary layer cannot be reached, or is reached only after a time interval much longer than determined experimentally.

Consider Eq. (24) in greater detail. When the concentration at the reaction surface reaches the limit value C_{Si}^{int} max, the reaction flow $r_0\psi$ is equal to the diffusive flow $D\,C_{Si}^{int}\,\max/\delta$. If the concentration is too low, then the diffusive flow is too high. As noted above, the boundary layer thickness can vary only by a factor of 4 or 5, depending on the hypotheses adopted. Saturation would be obtained only with a much lower diffusion coefficient (lower by a factor of 100 or more). In the Stokes–Einstein model, this would require silicon diffusion in the form of colloidal particles with a radius exceeding 35 nm. However, since these particles were not found in solution (only minor differences were noted between the filtered and ultrafiltered solutions in Table 3), this would imply that these entities were depolymerized within the same time frame as diffusion through the boundary layer. Modifying the diffusion coefficient by a factor of 100 would also modify the time constant t_1, which would thus be about 30 s: saturation would occur in 1 or 2 min. Assuming the particles were decomposed at the rate r_0, they would disappear in about ten minutes – substantially longer than t_1.

Another model could be considered, in which glass alteration is not homogeneous. The sodium borosilicate phase diagram [36] includes a miscibility gap for (Si, B, Na) glass with a liquidus (about 450–500°C) that is low enough compared with the vitreous transition temperature to result in heterogeneous glasses. The thermodynamics of the liquid above the transition point would conserve a trace of the interactions leading to this separation, resulting in a non-uniform distribution of B_2O_3 and SiO_2 that would favor the formation of molecular-scale groups. It can be imagined that fast alteration could dissolve the boron-enriched zones, leaving behind a tenuous silicon network that would dissolve more slowly. This structure would be on the scale of the glass, i.e. on the order of molecular dimensions. In this porous network, the diffusion coefficient could possibly drop sufficiently to allow saturation. This model is unlikely, however, since the Landau–Placzek ratio determined for the (Si, B, Na) glass (60) is nearly the same as for silica (50), and since no heterogeneities exceeding 50 Å were observed. Moreover, the experiments at 0.1 cm^{-1} showed relatively high silicon/boron congruence during the initial alteration phase, in contradiction with the assumed tenuous silica network arising from preferential release of boron.

These calculations have shown no obstacles to diffusion in solution that could account for local saturation with respect to amorphous silica. The most likely hypothesis for the formation of the gel layer at the glass/solution interface is local silica reorganization by a dynamic hydrolysis/condensation process. This hypothesis is discussed in the next section.

4.2.2. Exchange dynamics at the reaction interface

Relating the formation of the gel to the macroscopic notion of a solubility product thus cannot account for silicon retention over time at the glass/gel reaction interface. This reveals the limits of a purely thermodynamic approach that does not address the dynamics of exchange phenomena at the interface. A simple

calculation taking into account the reverse reaction of silicon recondensation can be envisaged. Silicon release would be controlled by the initial glass dissolution kinetics (r_0), while recondensation may be assumed to depend on the dissolved silicon concentration in the homogeneous solution. Silicon diffusion in the water is therefore assumed to occur quickly, and recondensation may occur at any point on the glass surface.

Steady-state conditions will occur in solution when the concentration of silicon remains constant. This steady state reflects only the equal flows of hydrolysis and recondensation (pseudo-reversibility) and does not, of course, correspond to an equilibrium between the dissolving initial (glass) phase and solution. This approach converges with the hypotheses formulated in the scope of Monte-Carlo simulations of borosilicate glass alteration, but remains macroscopic [37]; it does not take local effective probabilities into account.

The balance equation for the dissolution/recondensation kinetics is the following:

$$\frac{dC_{Si}}{dt} = r_0\psi\frac{S}{V} - k_r\frac{S}{V}C_{Si}, \tag{40}$$

where the product $k_r(S/V)$ defines a kinetic constant of recondensation (in s^{-1}). This is a 'global quantity' that does not allow for the greater silicon redeposition surface area, which undoubtedly increases as the silica gel is formed. The steady-state silicon regime ($dC_{Si}/dt = 0$) is defined by the $r_0\psi/k_r$ ratio.

The solution to this differential equation takes the following form:

$$C_{Si} = \frac{r_0\psi}{k_r}\left[1 - \exp\left(-k_r\frac{S}{V}t\right)\right], \tag{41}$$

where k_r can be determined for $t \to \infty$ since in this case $C_{Si} = C^*_{Si} = 320$ mg l^{-1} at pH 9. The mean recondensation frequency $k_r(S/V)$ is 2×10^{-5} s^{-1}.

The concentrations calculated from the balance equation are in very satisfactory agreement with the measured concentrations (Fig. 7). It should be noted that the balance equation merely reflects the validity of a $(1 - C_{Si}/C^*_{Si})$ law to account for the behavior of silicon, and silicon alone.

This calculation also shows that global, macroscopic values (the solution was assumed to be homogeneous) are sufficient to account for silicon retention at the reaction interface until saturation occurs with respect to amorphous silica. It is therefore unnecessary to take into account limited silicon diffusion, liable to result in locally higher concentrations than in the homogeneous solution, in order to describe the gel formation. This probably implies that at least until the solution becomes saturated with silicon, a silicon atom has a strong possibility of passing through the homogeneous solution before recondensing. It remains to be seen whether this silicon behavior, which seems to be verified up to the point at which saturation occurs, can be extrapolated over time in saturated media. Additional work should address this issue.

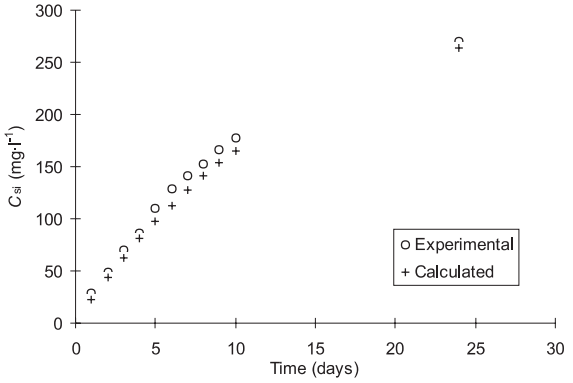

Fig. 7. Dissolved silicon concentration measured in solution versus time at $S/V = 4$ cm^{-1} compared with values calculated using a local dynamic model.

5. General conclusion

This investigation of a ternary (Si, B, Na) glass demonstrates that the driving force behind the alteration of this glass cannot be defined by a deviation from saturation, and that alteration does not stop when saturation occurs. The drop in the glass alteration rate at advanced stages of the reaction can be correlated with the formation of a gel with protective properties that seem to depend on the rate at which hydrolyzed species recondense (dynamic percolation). Although these conclusions are based on a simple system, they are corroborated by recent work with more complex glass compositions [22,28–30].

This experimental work also shows that classic chemical thermodynamics, based on the idea that statistical averages are representative of average microscopic behavior, cannot account for the glass alteration kinetics, primarily because the gel that forms at the glass/solution interface limits material transfers. It is therefore necessary to investigate the alteration film formation mechanisms at microscopic scale, and the effects of microscopic behavior on surface structure.

Acknowledgements

The authors are grateful to the French National Radioactive Waste Management Agency (ANDRA) for its financial support, to Dr Pelous of the Glass Laboratory at the University of Montpellier II (France) for

acquisition and processing of the light scattering spectra, and to Professor Grambow of the Nantes School of Mines (France) for his informal contribution to this work, notably through numerous discussions.

Appendix A. The shrinking core model

Symbols and units

R_0	mean initial radius of a sphere (cm)
R_i	mean radius of a sphere at time interval i (cm)
S_0	initial geometric surface area (cm^2)
S_i	geometric surface area at time interval i (cm^2)
m_0	initial powder mass (g)
m_i	powder mass at time interval i (g)
C_B	boron concentration (mg l^{-1})
C_j	concentration of species j (mg l^{-1})
X_B	boron mass fraction in the glass
X_j	j mass fraction in the glass
$(AG\%)$	mass percentage of altered glass
V	solution volume (ml)
S_i^{BET}/V_i	ratio of glass surface area to solution volume at time interval i (cm^{-1})
ρ	liquid density (g cm^{-3})
L	shape factor

A.1. Description

In the case of samples that are subject to significant relative mass alteration (typically more than 10%), the S/V ratio used to calculate the normalized mass loss must be corrected over time. This correction is implemented by means of a 'shrinking core' model in which the powder grains are considered as spheres.

At time interval i, the geometric surface area of the powder is

$$S_i = 4\pi N_{sph} R_i^2. \tag{A.1}$$

The number of spheres N_{sph} is defined by the following relation:

$$N_{sph} = \frac{3m_0}{4\pi R_0^3 \rho}. \tag{A.2}$$

Eq. (A.1) then becomes

$$S_i = \frac{3m_0 R_i^2}{\rho R_0^3}. \tag{A.3}$$

The unaltered powder mass m_i at time interval i is related to R_i by the following expression:

$$m_i = 4/3 N_{sph} \pi R_i^3. \tag{A.4}$$

Substituting the m_0 and R_0 term for N_{sph} in Eq. (A.4) gives

$$m_i = m_0 \frac{R_i^3}{R_0^3}. \tag{A.5}$$

The mean grain radius at time interval i is therefore

$$R_i = \left(\frac{m_i}{m_0}\right)^{1/3} R_0. \tag{A.6}$$

The m_i/m_0 mass ratio can easily be correlated with the mass percentage of altered glass determined experimentally from the concentrations in solution of an alteration tracer element (boron in this study). Thus

$$R_i = \left(\frac{100 - (AG\%)}{100}\right)^{1/3} R_0. \tag{A.7}$$

The altered glass mass percentage $(AG\%)$ is defined by the following relation:

$$AG\% = 10^{-4} \frac{C_B V}{m_0 X_B}. \tag{A.8}$$

The geometric surface area of the powder at time interval i, based on Eqs. (A.3) and (A.7), is then

$$S_i = \left(\frac{100 - (AG\%)}{100}\right)^{2/3} \frac{3m_0}{R_0}. \tag{A.9}$$

The geometric surface area S_i is recalculated at each time interval i from Eq. (A.8) using the shape factor L relating the geometric surface area to the BET surface area (L is assumed to remain constant during glass alteration). Thus

$$S_i^{BET} = LS_i, \tag{A.10}$$

where

$$L = \frac{S_0^{BET}}{S_0}. \tag{A.11}$$

The mass loss of element j calculated at time interval $i+1$ is then expressed as follows:

$$NL(j)^{i+1} = 10^{-2} \frac{C(j)^{i+1}}{\frac{S_i^{BET}}{V_i} X_j}. \tag{A.12}$$

References

[1] C.D. Byers, M.J. Jercinovic, R.C. Ewing, K. Keil, Scientific Basis for Nuclear Waste Management VIII, Mater. Res. Soc. Symp. Proc. 84 (1985) 67.
[2] J.L. Crovisier, B. Fritz, B. Grambow, J.P. Eberhart, Scientific Basis for Nuclear Waste Management IX, Mater. Res. Soc. Symp. Proc. 50 (1985) 273.
[3] J.L. Crovisier, H. Atassi, V. Daux, J. Honnorez, J.C. Petit, J.P. Eberhart, Scientific Basis for Nuclear Waste Management XII, Mater. Res. Soc. Symp. Proc. 127 (1989) 41.

[4] J.L. Crovisier, J. Honnorez, B. Fritz, J.C. Petit, Appl. Geochem. (Suppl. 1) (1992) 55.
[5] G. Berger, J. Schott, M. Loubet, Earth Planet. Sci. Lett. 84 (1987) 431.
[6] C. Guy, PhD thesis, University of Toulouse, France, 1989, p. 188.
[7] T. Advocat, J.L. Crovisier, E.Y. Vernaz, G. Ehret, H. Charpentier, Scientific Basis for Nuclear Waste Management XIV, Mater. Res. Soc. Symp. Proc. 212 (1991) 57.
[8] E.Y. Vernaz, J.L. Dussossoy, Appl. Geochem. (Suppl. 1) (1992) 13.
[9] Z. Boksay, G. Bouquet, S. Dobos, Phys. Chem. Glasses 9 (1968) 69.
[10] J.H. Thomassin, PhD thesis, Université d'Orléans, France, 1984, p. 215.
[11] M.J. Jercinovic, K. Keil, M.R. Smith, R.A. Schmitt, Geochim. Cosmochim. Acta 54 (1990) 2679.
[12] G. Berger, C. Claparols, C. Guy, V. Daux, Geochim. Cosmochim. Acta 58 (1994) 4875.
[13] V. Daux, C. Guy, T. Advocat, J.L. Crovisier, P. Stille, Chem. Geol. 142 (1997) 109.
[14] B. Grambow, Scientific Basis for Nuclear Waste Management VIII, Mater. Res. Soc. Symp. Proc. 44 (1985) 15.
[15] T. Advocat, J.L. Chouchan, J.L. Crovisier, C. Guy, V. Daux, C. Jégou, S. Gin, E.Y. Vernaz, Scientific Basis for Nuclear Waste Management XXI, Mater. Res. Soc. Symp. Proc. 506 (1998) 63.
[16] B.P. McGrail, W.L. Ebert, A.J. Bakel, D.K. Peeler, J. Nucl. Mater. 249 (1997) 175.
[17] P.K. Abraitis, B.P. McGrail, D.P. Trivedi, Scientific basis for nuclear waste management XXII, Mater. Res. Soc. Symp. Proc. 556 (1999).
[18] P. Aagaard, H.C. Helgeson, Am. J. Sci. 282 (1982) 237.
[19] W.L. Bourcier, D.W. Pfeiffer, K.G. Knauss, K.D. McKeegan, D.K. Smith, Scientific Basis for Nuclear Waste Management, Mater. Res. Soc. Symp. Proc. 176 (1990) 209.
[20] W.L. Bourcier, S.A. Carroll, B.L. Phillips, Scientific Basis for Nuclear Waste Management XXI, Mater. Res. Soc. Symp. Proc. 333 (1994) 507.
[21] S. Xing, C. Buechele, I.L. Pegg, Scientific Basis for Nuclear Waste Management, Mater. Res. Soc. Symp. Proc. 333 (1994) 541.
[22] C. Jégou, PhD thesis, Université de Montpellier, France, 1998, p. 207.
[23] Kadona et al., Phys. Chem. Glasses 35 (1) (1994).
[24] T. Advocat, PhD thesis, Université Louis Pasteur, Strasbourg, France, 1991.
[25] A. Paul, J. Mater. Sci. 12 (1977) 2246.
[26] C.M. Jantzen, M.J. Plodinec, J. Non-Cryst. Solids 67 (1984) 2074.
[27] F. Delage, F. Larché, E. Vernaz, Scientific Basis for Nuclear Waste Management XVI, Mater. Res. Soc. Symp. Proc. 294 (1993) 171.
[28] S. Gin, C. Jégou, E.Y. Vernaz, Use of orthophosphate complexing agents to investigate mechanisms limiting the alteration kinetics of French SON 68 nuclear glass, Appl. Geochem. (2000) in press.
[29] S. Gin, C. Jégou, E.Y. Vernaz, F. Larché, in: International Congress on Glass XVIII, The American Ceramic Society (July 1998), 1999.
[30] S. Gin, P. Jollivet, J.P. Mestre, M. Jullien, C. Pozo, French SON 68 nuclear glass alteration mechanisms on contact with clay media, Appl. Geochem. (submitted).
[31] R.B. Bird, W.E. Stewart, E.N. Lightfoot, Transport Phenomena, Wiley, New York, 1960.
[32] D.R. Lide (Ed.), CRC Handbook of Physics and Chemistry, 74th Ed., CRC, Boca Raton, FL, 1993, pp. 6–10.
[33] R.K. Iler, The Chemistry of Silica, Wiley, New York, 1979, p. 866.
[34] J.D. Rimstidt, H.L. Barnes, Geochim. Cosmochim. Acta 44 (1980) 1683.
[35] J., Philibert, A. Vignes, Y. Bréchet, P. Combrade, Métallurgie, du minerai au matériau, Masson, Paris, 1998.
[36] W. Haller, D.H. Blackburn, F.E. Wagstaff, J. Charles, J. Am. Ceram. Soc. 53 (1970) 34.
[37] F. Devreux, P. Barboux, B. Sapoval, CEA/Valrhô Summer Session Proceedings, Méjannes-le-Clap, September 1997, France, 1998.